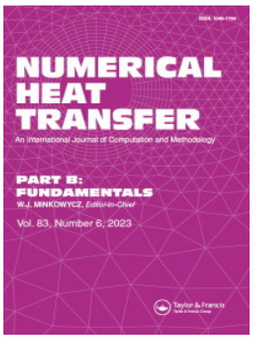

Taylor & Francis
Taylor & Francis Group

Numerical Heat Transfer, Part B: Fundamentals
An International Journal of Computation and Methodology

ISSN: (Print) (Online) Journal homepage: https://www.tandfonline.com/loi/unhb20

An alternative full multigrid SIMPLEC approach for the incompressible Navier–Stokes equations

Jean Michael Borges de Oliveira, Luciano Kiyoshi Araki, Marcio Augusto Villela Pinto & Simone de Fátima Tomazzoni Gonçalves

To cite this article: Jean Michael Borges de Oliveira, Luciano Kiyoshi Araki, Marcio Augusto Villela Pinto & Simone de Fátima Tomazzoni Gonçalves (2023) An alternative full multigrid SIMPLEC approach for the incompressible Navier–Stokes equations, Numerical Heat Transfer, Part B: Fundamentals, 83:6, 410-432, DOI: 10.1080/10407790.2023.2167752

To link to this article: https://doi.org/10.1080/10407790.2023.2167752

NUMERICAL HEAT TRANSFER, PART B: FUNDAMENTALS
2023, VOL. 83, NO. 6, 410–432
https://doi.org/10.1080/10407790.2023.2167752

An alternative full multigrid SIMPLEC approach for the incompressible Navier–Stokes equations

Jean Michael Borges de Oliveira[a], Luciano Kiyoshi Araki[b], Marcio Augusto Villela Pinto[b], and Simone de Fátima Tomazzoni Gonçalves[b]

[a]Graduate Program in Numerical Methods in Engineering, Federal University of Parana, Curitiba, Brazil; [b]Department of Mechanical Engineering, Federal University of Parana, Curitiba, Brazil

ABSTRACT

An alternative approach to solve the steady-state incompressible Navier–Stokes equations using the multigrid (MG) method is presented. The mathematical model is discretized using the finite volume method with second-order approximation schemes in a uniform collocated (nonstaggered) grid. MG is employed through a full approximation scheme-full MG algorithm based on V-cycles. Pressure-velocity coupling is ensured by means of a developed modified SIMPLEC algorithm which uses independent V-cycles for relaxing the pressure-correction and momentum equations. The coarser grids are used only internally in these cycles. All other original SIMPLEC steps can be performed only on the finest grid of the current full MG level. The model problem of the lid-driven flow in the unitary square cavity is used for the tests of the numerical model. Computational performance is measured through error and residual decays and execution times. Good performances were obtained for a wide range of Reynolds numbers, with speedups of orders as high as $O(10^3)$. Linear relationships between execution times and grid sizes were observed for low and high Re values ($Re = 0.1, 1, 10, 2,500, 3,200, 5,000$, and 7,500). For intermediate Re values ($Re = 100, 400$, and 1,000), the linear trend was observed from more refined grids (512^2 onwards).

ARTICLE HISTORY
Received 27 September 2022
Revised 28 November 2022
Accepted 5 January 2023

KEYWORDS
Finite volume method; full-multigrid; Navier–Stokes equations; SIMPLEC

1. Introduction

In the last decades, obtaining accurate numerical solutions of the Navier–Stokes equations for different flow problems has been the main objective of several works in the computational fluid dynamics (CFD) area [1–4]. However, the use of conventional (or standard) iterative methods for solving these and other partial differential equations (PDEs) problems may result in slow convergence rates and high computational costs when solutions on high-resolution meshes are required and/or the complexity of the numerical models increases [2,5]. In this sense, multigrid (MG) methods have been widely used to accelerate the converge of traditional iterative solvers used for the large algebraic systems associated with these kind of problems.

In the case of the incompressible Navier–Stokes equations, there is no explicit equation for the pressure as the mass conservation is expressed in terms of the velocity divergent-free relation. Therefore, the problem of decoupling between velocities and pressure arises and, to overcome it, some method responsible for ensuring the pressure-velocity coupling is required. The so-called pressure-correction methods are widely used for this purpose. Among these methods, the

CONTACT Jean Michael Borges de Oliveira jmboliveira86@gmail.com Graduate Program in Numerical Methods in Engineering, Federal University of Parana, Curitiba 80060-000, Brazil.

SIMPLE family [6] certainly stands out, although other types of pressure-correction methods are also commonly used, as the one employed in Anunciação *et al.* [7].

In the last decades, several researchers have studied different ways of implementing MG methods together with SIMPLE-like methods to solve the incompressible Navier–Stokes equations. In the following paragraphs, some of these works are briefly reviewed.

After the initial works of Fedorenko [8] and Bakhvalov [9], which debuted the MG methods, and the work of Brandt [10], which set their theoretical background, one of the first studies to use MG to solve the Navier–Stokes equations was the one from Ghia *et al.* [1]. However, no coupling method was employed as the vorticity-stream function formulation of the equations was used. This early work presented impressive results in implementing the full approximation scheme-full multigrid (FAS-FMG) algorithm [11] for simulations involving the classical square lid-driven cavity problem for Reynolds number as high as 10,000 and fine grids up to 256×256 volumes. For $Re = 1,000$ in a 129×129 grid, for example, the processing times required for the solutions to converge were reduced by an hour or more in previous works to 1.5 min.

To this day, the work of Ferziger *et al.* [12] stands out as one of the pioneers in the use of MG in conjunction with the SIMPLE method for the pressure-velocity coupling of the incompressible Navier–Stokes equations. In this study, the finite volume method (FVM) was used for the discretization of the equations and, with respect to the MG method, the FAS algorithm was employed in conjunction with V-cycles and nested iteration. Good results were observed for the problem of the flow over the backward facing step, with the computational times increasing almost linearly in relation to the number of variables.

Other studies that employ the MG-SIMPLE-like formulations are the ones by Kumar *et al.* [13] and Roy *et al.* [14]. The two papers present detailed derivations of the numerical models and algorithms. Both use the FVM to discretize de equations with the collocated arrangement of the variables, but different schemes of pressure-velocity coupling are employed in each one. The lid-driven flow in the square cavity model problem is also used for the simulation tests in the two studies. In Kumar *et al.* [13], the numerical model is based on the MG-SIMPLEC formulation, in which the MG was employed in terms of the FAS scheme and V-cycles. However, instead of measuring the computational performance of the method, the main objective of that paper was to generate accurate solutions of the cavity problem for some Reynolds numbers within the range of 1,000–10,000.

The numerical model of Roy *et al.* [14] is built based on ideas that are similar to those found in Lien and Leschziner [5], with the difference that in the earlier work a nonorthogonal scheme is used for the discretization of the equations. In Roy *et al.* [14], a parallel MG-SIMPLE solver is presented, although the full development of the serial numerical model is first presented in detail. MG is implemented in terms of the FAS-FMG algorithm and V-cycles. The parallel model achieves optimal MG efficiency, with the computing time increasing linearly with the number of variables. Almost linear scalability (or speedup) of the parallel version in relation to the serial one (in a 512×512 grid) is also achieved. In addition, benchmark solutions of the cavity problem for Reynolds numbers over a range from 400 to 7,500 are presented.

In all these works, the SIMPLE-like schemes executed on the coarse grids of the MG are based on modified versions of the fine grid conservation equations, also called "coarse grid correction equations" [14]. The modified coarse grid momentum equations are driven by the finer grid residuals, which originated from nonconverged solutions. These solutions together with the respective residuals are restricted from the finer grid in a FAS fashion. As the corrections for the pressure are linear, no pressure is restricted from the finer grid and the coarse grid momentum equations are based on pressure-correction gradients instead of simple pressure ones. After solving the coarse grid momentum equations, the intermediate velocity and pressure-correction fields must be corrected. For this purpose, the continuity equation is transformed into a modified equation of "corrections for pressure-corrections" which, after being calculated, are used to correct the

pressure-correction and velocity fields. Throughout this article, this approach will be referred to as the standard approach for MG-SIMPLE-like schemes.

During the assembly of the momentum equations, the values of the velocities on the faces of the volumes are necessary. As in the collocated arrangement the variables are originally calculated on volumes centroids, the momentum interpolation method (MIM) of Rhie and Chow [15] is generally used to approximate the velocities on the faces. In the standard MG-SIMPLE-like approach, this method also must be modified on coarse grids to take into account the additional terms restricted from the finer grid. The calculation of face velocities plays an important role in SIMPLE-like pressure-correction methods and the incorrect application of MIM (or its variants) can lead to slow convergence of the iteration scheme, or even divergence [16]. Another issue worth commenting is the setting of boundary conditions for the equation that corresponds to the continuity equation in coarse grids. Since this equation is an equation of "corrections for pressure-corrections" it can be tricky to assign physical meaning to the independent variables when defining these conditions.

Another important work that uses the MG-SIMPLE formulation scheme is the one by Yan *et al.* [17]. In this study, the authors also point out some undesirable features of the standard approach. It is stated that the initially restricted mass fluxes through the faces of the coarse grid volumes may not match the restricted velocities balances in the corresponding centroids. According to the authors, these mismatches can lead to instability and decreased acceleration efficiency or even divergence. In that work, it is proposed an alternative modified MG-SIMPLE algorithm in which the residuals are the only information restricted to coarser grids. All other initial quantities on coarse grids are taken from the previous cycle. The new algorithm achieved notable performance when compared to previous works, presenting speedups with two orders of magnitude and a linear increase in execution time in relation to the number of variables; that is, optimal MG efficiency.

Considering all these issues regarding the standard approach, the main objective of this article is to propose an alternative and simpler approach for the construction of numerical models based on the MG-SIMPLEC formulation to solve the incompressible steady-state Navier–Stokes equations on collocated grids. In this approach, the MG is employed by means of an FMG algorithm and the original SIMPLEC algorithm is executed practically without modifications and only on the finest grid of each FMG level. The only differences are that, in the steps corresponding to the resolution of their associated linear systems, the momentum equations and the pressure-correction equation are solved by means of independent V-cycles.

The problem of the lid-driven flow in the unitary square cavity [1,18] is used for the verification tests of the numerical model built from the proposed approach. This problem has great importance in CFD and has been used by many researchers for testings and verifications of their new methods and techniques due to its simplicity and richness of fluid flows phenomena it contains [19].

As a secondary objective, it is also intended that the numerical model achieves the expected MG efficiency rule [10,14]: the computational effort, in terms of CPU times, must increase following an $O(N)$ trend, where N is the number of grid volumes. In most works in the literature, the range of Reynolds numbers (Re) employed in MG performance tests for the square lid-driven cavity problem is limited. Higher values ($Re \geq 1,000$) are rarely found in such tests, generally the most common tested values are 100, 400, and 1,000. Therefore, it is desired that, in this work, the efficiency rule is reached for a varied range of Re, but mainly for higher values.

This article is divided as follows: in Section 2, the discretization of the governing equations alone is presented; in Section 3, the proposed MG-SIMPLEC approach is presented and employed to construct a representative numerical model; Section 4 presents and discusses the results obtained from the application of the developed model for simulations involving the square lid-driven cavity problem; the conclusions of the present work are discussed in Section 5.

2. Mathematical and numerical models

2.1. Mathematical model

Considering the two-dimensional laminar steady-state flow of an incompressible Newtonian fluid, without heat transfers, the conservations of momentum and mass, representing the Navier–Stokes equations, can be written as follows [18]:

$$\frac{\partial}{\partial x}(u^2)+\frac{\partial}{\partial y}(uv)=-\frac{1}{\rho}\frac{\partial p}{\partial x}+\nu\left(\frac{\partial^2 u}{\partial x^2}+\frac{\partial^2 u}{\partial y^2}\right), \tag{1}$$

$$\frac{\partial}{\partial y}(v^2)+\frac{\partial}{\partial x}(vu)=-\frac{1}{\rho}\frac{\partial p}{\partial y}+\nu\left(\frac{\partial^2 v}{\partial x^2}+\frac{\partial^2 v}{\partial y^2}\right)+S, \tag{2}$$

$$\frac{\partial u}{\partial x}+\frac{\partial v}{\partial y}=0, \tag{3}$$

where u and v are the velocity vector components (m/s) in x and y directions, p (Pa) is the pressure, ρ (kg/m^3) and ν (m^2/s) are the density and kinematic viscosity of the fluid, respectively. It is assumed that ρ and ν have constant values in space and time in all simulations. Furthermore, the density is taken as unitary, $\rho = 1$ kg/m^3, and the viscosity is set to calculate the desired input Reynolds number, as in Marchi *et al.* [18].

The source term S of the momentum conservation in the y direction, Eq. (2), is related to the model problems used for the numerical tests. Two variants of the flow problem in the square cavity are used: the classical problem [18,20], for which there is no analytical solution, and the problem with a manufactured analytical solution by Shih *et al.* [21].

A depiction of the unitary square cavity is given in Figure 1. For both model problems, the velocities u and v are defined as zero on the side and bottom walls, as well as v on the top lid. In the classical problem, the top lid horizontal velocity, u, is unitary, that is: $u(x,1) = u_T(x) = 1$; and in the problem of Shih *et al.* [21] it is given by:

$$u(x,1)=u_T(x)=16\left(x^4-2x^3+x^2\right). \tag{4}$$

The manufactured analytical solutions of u and v are given by:

$$u(x,y)=8\left(x^4-2x^3+x^2\right)\left(4y^3-2y\right), \tag{5}$$

$$v(x,y)=-8\left(4x^3-6x^2+2x\right)\left(y^3-2y\right). \tag{6}$$

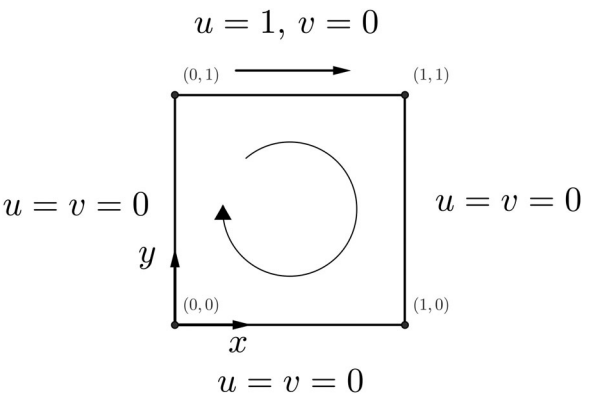

Figure 1. Boundary conditions in the square cavity for the two considered model problems.

The expressions for the pressure analytical solution, $p(x, y)$, and for the source term S are quite long and, therefore, may be checked directly in the article. In the classical problem, the source term is null.

2.2. Discretization

The mathematical model is discretized using the FVM [22]. In this method, the discrete version of the initial continuous domain is divided into control volumes, which compose a grid so that each point on the grid is surrounded by only one volume and there is no overlapping between volumes. A typical central volume, whose central point is P, and the adjacent volumes are depicted in Figure 2. The central points of the surrounding volumes are indicated by W, E, S, and N, representing neighboring volumes west, east, south, and north, respectively. The intersecting faces between these volumes and the central volume P are indicated by the corresponding lowercase letters. The grid adopted here has the same characteristics as the one shown in the figure; that is, a uniform orthogonal grid with a collocated (nonstaggered) arrangement is used and the nodal points are located in the centroid of each volume.

After the discretization of the domain, the governing equations are integrated over each control volume. The integrals of the space derivatives are evaluated through the corresponding fluxes across the volumes' faces. These fluxes are approximated by discrete differences involving neighboring points. In this work, the diffusive fluxes are approximated by central difference schemes (CDS), with second-order accuracy, and the convective fluxes are approximated by upwind difference schemes (UDS) with deferred correction [23] to also obtain second-order approximations. The pressure gradients, evaluated in the volumes centroids, are also approximated by CDS expressions. In the case of the problem with the manufactured solution, the integral of the source term, $S(x, y)$, over the control volume is approximated with the midpoint rule [24]. For more information on these approximation schemes and techniques, the books by Maliska [22] and Ferziger and Perić [25] can be consulted.

A pseudo-time-marching scheme is also used to improve the convergence of the numerical models. In this scheme, time is used as a relaxation parameter that helps solutions to reach the steady-state from a pseudo-transient state in an iterative process. Therefore, in the discretization process, the time derivatives $\partial u/\partial t$ and $\partial v/\partial t$ are included on the left side of the Eqs. (1) and (2),

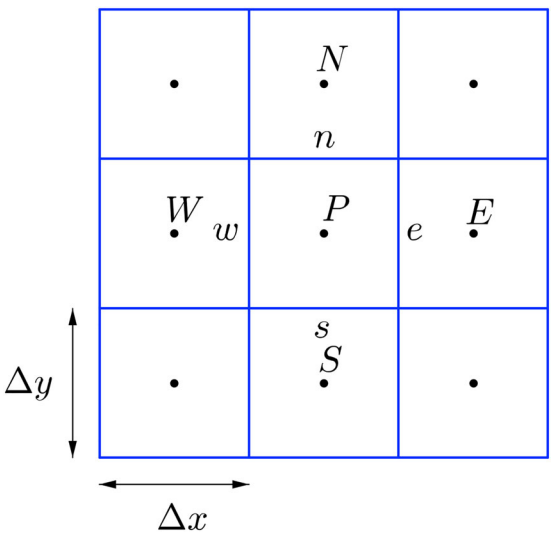

Figure 2. Typical control volumes surrounding the grid points.

respectively. These derivatives are approximated with an implicit Euler method. This technique is equivalent to the use of under-relaxation in the resulting algebraic equations and, therefore, increases the diagonal dominance of the associated coefficient matrices. Furthermore, as the governing equations are nonlinear, the iterative pseudo-time-marching scheme is also a way to deal with the nonlinearities [22], as it uses successive linearization of the equations to generate linear systems [25].

The discretized approximated momentum equations can be written as:

$$A_P^V u_P = \sum_{nb} A_{nb}^V u_{nb} - \frac{p_E - p_W}{2}\Delta y + \bar{S}_P^u, \tag{7}$$

$$A_P^V v_P = \sum_{nb} A_{nb}^V v_{nb} - \frac{p_N - p_S}{2}\Delta x + \bar{S}_P^v, \tag{8}$$

where the index nb runs over the neighboring points W, S, E, and N. The coefficients A^V are the same for both velocity components u and v and also can be checked in Maliska [22] and Ferziger and Perić [25]. The pressure differences in Eqs. (7) and (8) result from the pressure gradients approximations on the central point P using central schemes (cf. Figure 2). The source terms $\bar{S}^u$ and $\bar{S}^v$ contain the terms related to the deferred corretion and to the pseudo-time-marching scheme. Additionally, the case of the problem with manufactured solution, $\bar{S}^v$ also contains the source term S (Eq. (2)).

The last two terms of Eqs. (7) and (8) are actually added together and incorporated into the respective independent terms of the equations, which are then given by:

$$S_P^u = -\frac{p_E - p_W}{2}\Delta y + \bar{S}_P^u, \tag{9}$$

$$S_P^v = -\frac{p_N - p_S}{2}\Delta x + \bar{S}_P^v. \tag{10}$$

After the integration of Eq. (3), mass conservation is described in terms of mass flux balances through control volumes faces, according to:

$$\dot{M}_e - \dot{M}_w + \dot{M}_n - \dot{M}_s = 0, \tag{11}$$

where the mass fluxes $M_f, f = s, w, e, n,$ are calculated using relations similar to the following:

$$\dot{M}_e = \rho u_e \Delta y, \tag{12}$$

$$\dot{M}_n = \rho v_n \Delta x. \tag{13}$$

These fluxes are used as linearizations of the nonlinear convective terms in Eqs. (1) and (2). As will be shown, they are always calculated using the velocity field from the previous (external) iteration and are then used in the calculation of the new velocity field of the current iteration. In Eqs. (7) and (8), they are used to compose the coefficients A_P^V and A_{nb}^V.

2.3. Standard SIMPLEC method

To transform Eq. (11) in an equation for pressure, the SIMPLEC-like methods assume that the solutions of the momentum equations produce an intermediate velocity field, indicated by u^* and v^*, that does not satisfy the continuity equation; the corresponding intermediate pressure field is indicated by p^*. To obtain divergent-free velocity and pressure fields, corrections u', v', and p' for the intermediate fields are introduced so that the corrected quantities $\phi_\tau = \phi_\tau^* + \phi_\tau'$, for $\phi = u, v, p$, satisfy both the continuity and momentum equations. The index τ indicates the grid location of the

variables and may assume node values, $\tau = P,\ W,\ E,\ S,\ N$, or face values, $\tau = w,\ e,\ s,\ n$. In the SIMPLEC method, the relationships between velocities and pressure-corrections take the following forms:

$$u_P = u_P^* - d_P^u\left(p'_e - p'_w\right), \tag{14}$$

$$u_e = u_e^* - d_e^u\left(p'_E - p'_P\right), \tag{15}$$

where the SIMPLEC coefficients, d_P^u and d_e^u, are given by:

$$d_P^u = \left(\frac{\Delta y}{A_P^V - \sum_{nb} A_{nb}^V}\right)_P, \tag{16}$$

$$d_e^u = \left(\frac{\Delta y}{A_P^V - \sum_{nb} A_{nb}^V}\right)_e. \tag{17}$$

The right side of the Eq. (17) may be obtained by a linear interpolation of the terms inside the parentheses involving the nodes adjacent to the e face, that is, nodes P and E.

According to the discretization techniques and approximations adopted in this work, these relations lead to the following fixed expressions for the SIMPLEC coefficients:

$$d_P^u = \frac{\Delta t}{\rho \Delta x}, \tag{18}$$

$$d_e^u = \frac{(d_P^u)_P + (d_P^u)_E}{2}, \tag{19}$$

where Δt is the time step for the pseudo-time-marching continuation. Relation of Eq. (19) is recommended by Maliska [22]. The values of the parameters Δx, Δy, and Δt are predefined by the discretization of the initial problem. Thus, the SIMPLEC coefficients may be calculated only once and stored during the execution of the method. Relations analogous to those of Eqs. (14)–(19) are used for the other nodes and faces.

The substitution of the correction expressions, similar to Eq. (15), in Eq. (11) generates the discretized pressure-correction equation, which can be written as:

$$A_P^p p'_P = \sum_{nb} A_{nb}^p\ p'_{nb} + S_P^p. \tag{20}$$

The coefficients A^p depend only on the SIMPLEC coefficients (their values can be found in Maliska [22] and Ferziger and Perić [25]), and thus, can also be calculated only once and stored. The independent term S^p contains the mass imbalance of the intermediate velocity components, which is given by:

$$\begin{aligned} S_P^p = \dot{m} &= -(\rho u_e^* \Delta y - \rho u_w^* \Delta y + \rho v_n^* \Delta x - \rho v_s^* \Delta x) \\ &= -\left(\dot{M}_e^* - \dot{M}_w^* + \dot{M}_n^* - \dot{M}_s^*\right). \end{aligned} \tag{21}$$

Thus, one way to ensure that the velocity field is divergent-free is to monitor S^p. This term is expected to tend to zero as the iterations progress.

The face velocities needed in Eq. (21) must be calculated using the intermediate velocity field obtained from the momentum equations. The method MIM of Rhie and Chow [15] is used here for this purpose. Instead of just linearly interpolating the face velocities, this method uses the momentum equations, Eqs. (7) and (8), evaluated on the nodes adjacent a certain face to compose the corresponding face velocity. The face velocity on the east interface, for example, is obtained by

interpolating Eq. (7) on nodes P and E, with the exception of pressure terms, giving [15,22]:

$$u_e = \frac{\left(\sum A^V_{nb} u^*_{nb}\right)_P + \left(\sum A^V_{nb} u^*_{nb}\right)_E + \frac{M_P + M_E}{\Delta t} u^0_e - 2(p^*_E - p^*_P)}{\left(A^V_P\right)_P + \left(A^V_P\right)_E}. \tag{22}$$

The other face velocities are obtained by similar relations. The iterative steps of the SIMPLEC method are represented in Algorithm 1.

Algorithm 1: SIMPLEC algorithm for Navier–Stokes equations.

1 Initialize the variables u, v, p, and p';
2 Calculate mass fluxes, Eqs. (12) and (13);
3 Calculate SIMPLEC coefficients (relations similar to Eqs. (16) and (17));
4 Calculate pressure coefficients A^p;
while *Stopping criterion is not satisfied* **do**
5 Calculate velocity coefficients A^V and independent terms S^u and S^v;
6 Solve the momentum equations, Eqs. (7) and (8), and obtain u^* and v^*;
7 Calculate face velocities u^*_e and v^*_n (relations similar to Eq. (22));
8 Calculate pressure-correction independent term S^p, Eq. (21);
9 Solve the pressure-correction equation, Eq. (20), and obtain p';
10 Correct the pressure field using the relation $p = p^* + p'$;
11 Correct nodal and face velocities with relations similar to Eqs. (14) and (15);
12 Correct mass fluxes applying velocity corrections on Eqs. (12) and (13);
13 Set $p^* = p$;
14 Return u, v, p.

3. Multigrid

Traditional iterative methods for solving linear systems of equations, like Gauss–Seidel and Jacobi methods, are efficient in eliminating only the oscillatory (or high frequency) components of the errors associated with the dependent variables. In general, they are not able to efficiently eliminate the smooth (or low frequency) error components. For this reason, these methods are often called smoothers, because they tend to smooth out the errors [26]. Thus, at the beginning of the iterative process a high convergence rate is observed and is associated with the rapid elimination of the oscillatory components. After some few iterations, there is a significant decrease in this rate, which is due to the slow elimination of low frequency components.

The error components that are seen as smooth on a fine grid become more oscillatory when represented on a coarser grid, that is, when the error is transferred to a coarser grid. Thus, it can be said that common iterative methods efficiently remove only the error components whose wavelengths are approximately comparable to the current grid spacing [2]. Therefore, to eliminate most of the frequencies of the error components, the main idea behind the MG methods is to use a set of coarser grids to smooth the corresponding oscillatory components of each one. The main features of the MG methods are briefly presented in the sequence. For a detailed description of these and all other standard MG topics covered in this section, the book by Trottenberg *et al.* [26] can be consulted.

3.1. Standard MG

The main ideas of the MG method are better described by a two grid system, consisting of a initial fine grid and a coarser one, indicated by Ω^h and Ω^{2h}, respectively. The superscript h is a representative measure of the of volumes lengths in the two coordinate directions, $h = \max(\Delta x, \Delta y)$. So, the coarsening ratio $q = 2$ is the standard value and the grid Ω^{2h} has twice the volumes in

each coordinate direction in relation to the fine grid. In this work, the grid is uniform [25] and composed of square volumes ($\Delta x = \Delta y$).

For nonlinear problems, the full approximation scheme (FAS) is more suitable; for the case of linear problems, the correction scheme (CS) is more appropriate. As the problem addressed in this work is fundamentally nonlinear, only the two-grid FAS scheme is (briefly) reviewed in Algorithm 2. The generic dependent variable ϕ can assume the values of u, v or p and the surrounding parentheses are a notation to indicate that the systems are nonlinear. The operator A^{2h}, in step (4), is obtained by rediscretization of the original problem [26]. The right-hand side of the equation in step (4) is computed once and kept fixed during the iterations in Ω^{2h}.

Algorithm 2: Two-grid full approximation scheme (FAS).

1. Relax ν_1^{ϕ} times $A^h(\phi^h) = f^h$ in Ω^h with initial estimate ϕ_0^h and obtain an intermediary solution ϕ^{h*};
2. Compute the residual $r^h = f^h - A^h(\phi^{h*})$ and restrict it to Ω^{2h}, $r^{2h} \leftarrow I_h^{2h} r^h$;
3. Restrict the intermediary solution ϕ^{h*} and define it as the initial estimate in Ω^{2h}, $\phi_0^{2h} \leftarrow I_h^{2h} \phi^{h*}$;
4. Solve $A^{2h}(\phi^{2h}) = A^{2h}(\phi_0^{2h}) + r^{2h}$ in Ω^{2h} with initial estimate ϕ_0^{2h} and obtain the solution ϕ^{2h};
5. Compute the error in Ω^{2h}, $e^{2h} = \phi^{2h} - \phi_0^{2h}$;
6. Prolong the error from Ω^{2h} and correct the intermediary solution in Ω^h, $\phi^h \leftarrow \phi^{h*} + I_{2h}^h e^{2h}$;
7. Relax ν_2^{ϕ} times $A^h(\phi^h) = f^h$ in Ω^h with initial estimate ϕ^h.

Instead of using just two grids, the FAS scheme is generally employed to a successive set of increasingly coarser grids, which are successively indicated by $\Omega^h, \Omega^{2h}, \Omega^{4h}, \ldots, \Omega^{Lh}$, where Ω^{Lh} indicates the coarsest possible grid. In this work, the dimension of Ω^{Lh} is 2^2 (2×2). The superscript L is a even integer given by $L = 2^{L_{\max}}$, where $L_{\max}$ is the maximum number of possible coarser grids obtained from a certain initial fine grid, Ω^h, when coarsening ratio $q = 2$ is employed.

The error being calculated in an intermediate grid $\Omega^{(2k)h}$ (k integer and $k \geq 1$) is related with the residual equation solution from the previous finer grid Ω^{kh}, that is already an equation for an error. The way grids with different spacing's are traversed defines a MG cycle and each grid in the cycle is also referred to as a level. Amongst the several types of existing cycles, the V-cycle [26] is perhaps the most simple and straightforward on the representation of the MG ideas.

For the V-cycle to be efficient, it is necessary that the information is transferred correctly from one grid to another. A restriction operator that is often used in conjunction with second-order finite volume models considers that properties in a coarse grid volume are obtained from summation expressions involving their values in the corresponding four finer grid volumes: variables and residuals are, respectively, calculated using the arithmetic mean and the direct sum of their values in the four finer grid volumes [25]. Mass fluxes are also restricted based on this idea, considering that a certain face of a coarse grid volume corresponds to two faces in the finer grid [2]. The bilinear interpolation operator [26] is used here for the prolongation of all coarse grid information. As the bilinear operator has order 2, the orders of the two transfer operators used are adequate in relation to the orders of the derivatives of the governing equations [27].

The most efficient form of the MG method is when nested V-cycles with different number of grid levels are used. The solution process starts solving the system in an initial coarse grid (which can be predefined or be the coarsest possible grid, Ω^{Lh}), the obtained solution is then prolonged as an initial estimative to the next finer grid and a V-cycle is executed there. After the execution, its solution (which can be intermediate or converged) is prolonged to the next finer grid as an initial estimative for a V-cycle that contains one level more than the previous one. This process is repeated until the initial finest grid is reached and from there, V-cycles involving $L_{\max}$ levels are executed until convergence of the original problem. This algorithm is called full multigrid (FMG). A representation of a FMG algorithm, with 4 grid levels, is shown in Figure 3. The dots between cycles indicate that multiple V-cycles can be executed before prolonging the solutions to the next

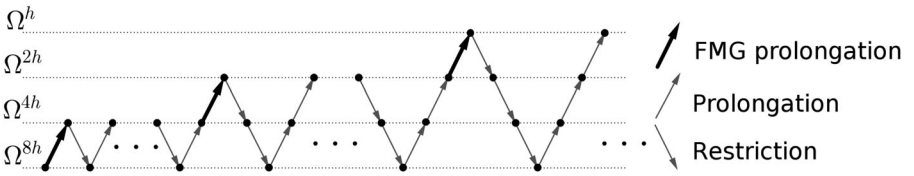

Figure 3. Representation of the FMG algorithm using V-cycles.

FMG level. A more detailed study on the number of V-cycles to be performed at each FMG level can be found at Thekale *et al.* [28]. The FMG algorithm is used in this work and all the V-cycles of all its levels go to the coarsest possible grid Ω^{Lh}.

3.2. Alternative FMG-SIMPLEC approach

As aforementioned, the MG approaches used in conjunction with SIMPLE-like methods are generally based on so-called coarse grid correction equations, which are modified versions of the momentum and continuity equations. On coarse grids, the momentum equations are based on pressure-correction gradients, instead of just pressure ones, and the continuity relation is transformed in an equation of corrections for pressure-corrections. Moreover, when calculating the face velocities, the MIM [15], or its variants, must be modified to also take into account the additional FAS restricted terms when interpolating Eq. (7) or Eq. (8) on the nodes adjacents to a specific volume face. The development of these approaches is not presented here, but can be seen in detail in Roy *et al.* [14].

Before presenting the scheme developed in this work, there are some points worth mentioning. In the discretized momentum equations on the fine grid, the pressure contribution is stored in the independent terms, Eqs. (9) and (10), together with the deferred correction terms and the pseudo-time-marching scheme terms. However, if a MG method is being used, the independent terms in intermediate coarse grids are used exclusively to store the FAS related terms; thus, they do not store pressure terms. So, if a system consisting only of the two momentum conservation equations is to be solved by a MG method, as in the case of Burgers equations [29], the only influence of pressure on the coarse grid equations are those that come implicitly in the restricted quantities (velocities, mass fluxes, and residuals).

Observing that, in the case of the Navier–Stokes equations, the most current pressure field can be kept fixed during the execution of a specific V-cycle to solve the momentum conservation equations. In this work, this cycle is called (u, v)-cycle and it is used in replacement of the single grid (SG) relaxations of the u and v systems in step (4) of Algorithm 1. To compute the nonlinear part of the coarse grid matrix coefficients, A_F^V ($F = S, W, P, E, N$), the most updated mass fluxes can also be kept fixed and restricted during the execution of the (u, v)-cycle, since they are corrected only through pressure-corrections.

In the case of the pressure-correction equation, it was already mentioned that the coefficients A^p, in Eq. (20), depend only on the SIMPLEC coefficients, which are fixed according to the discretization procedure employed here (Eqs. (18) and (19)). Therefore, these coefficients may be calculated only once and stored on each grid. The only term in Eq. (20) that depends directly on the velocities is the independent term, Eq. (21), which on coarse grids is also used exclusively to store the restricted terms from FAS. Therefore, instead of performing the singlegrid relaxation of the p' system in step (8) of Algorithm 1, a specific and independent pressure-correction V-cycle can also be used. This cycle will be called p-cycle here.

Similarly to what happens in the (u, v)-cycle, the last, and most updated, velocity field is also kept fixed during the executions of the p-cycle. If other discretization techniques and approximations are used for the governing equations and the SIMPLEC coefficients are not given by fixed expressions, like Eqs. (18) and (19). In that case, the fine grid fixed velocity field must also be restricted to calculate the SIMPLEC coefficients and, consequently, the pressure-correction coeffients A^p in the coarse grids of the p-cycle.

It is defined here that both (u, v)-cycle and p-cycle use the maximum number of grid levels from a given initial fine grid, that is, both have $L_{\max}$ coarser grids. However, the value of this parameter was chosen for convenience and not through a dedicated study to determine the optimal number of levels that should be used in each cycle. If a FMG algorithm is being used, this initial fine grid will be the finest grid of the current FMG level, which is indicated here by Ω^H to differentiate it from the initial finest grid of the problem, Ω^h. In this work, an alternative full-multigrid SIMPLEC (FMG-SIMPLEC) approach is proposed to solve the numerical problem on the finest grid, Ω^h. This approach is described in the following paragraphs.

On the local finest grid of each FMG level, Ω^H, the problem is solved by means of a modified SIMPLEC algorithm, which is called "Mod-SIMPLEC" in this work. In this algorithm, the momentum and pressure-correction systems, steps (4) and (8) of Algorithm 1, are solved using the (u, v)-cycle and the p-cycle, respectively. The numbers of times each of these cycles is executed, in steps (4) and (8), are indicated by γ_1 and γ_2, respectively. With the exception of these two steps, all other steps of the original SIMPLEC algorithm, such as calculating face velocities (by means of the MIM) or correcting velocity and pressure fields, are executed without modification in Mod-SIMPLEC and only on Ω^H.

Mod-SIMPLEC is always executed up to convergence on each FMG level and the obtained converged solutions are transferred as initial estimative to the next level by means of the FMG prolongation. This process is repeated until the last FMG level, whose finest grid is the initial grid Ω^h, is reached. Mod-SIMPLEC is also executed there until convergence of the initial problem systems.

The steps that correspond to the proposed approach are presented in Algorithm 3. As can be noted from steps (5) and (6), the coefficients of SIMPLEC and also of the pressure-correction equation are calculated only once and stored in each grid level. Mod-SIMPLEC comprises steps (7) to (15) within the innermost loop. In addition, only steps (8) and (11) involve different grid levels, all other steps are performed only on Ω^H. In step (8), the mass fluxes from Ω^H should also be restricted in the (u, v)-cycle, to assemble the coefficients A^V on coarse grids.

Algorithm 3: FMG based on a modified SIMPLEC algorithm

1 Execute Algorithm 1 on an initial coarse grid $\Omega^{(2l)h}$ up to convergence;
2 Prolong solutions u, v, and p to the next finer grid Ω^{lh};
3 $H \leftarrow lh$;
while $H \geq h$ **do**
4 Calculate mass fluxes, Eqs. (12) and (13), on Ω^H;
5 Calculate SIMPLEC coefficients (relations similar to Eqs. (16) and (17)) on Ω^H;
6 Calculate pressure coefficients A^p on Ω^H;
while *Convergence criterion on* Ω^H *is not satisfied* **do**
7 Calculate velocity coefficients A^V and independent terms S^u and S^V;
8 Execute γ_1 (u, v)-cycles to solve Eqs. (7) and (8) and obtain u^* and v^*;
9 Calculate face velocities u_e^* and v_n^* on Ω^H (relations similar to Eq. (22));
10 Calculate pressure-correction independent term S^p, Eq. (21), on Ω^H;
11 Execute γ_2 p-cycles to solve Eq. (20) and obtain p';
12 Correct the pressure field on Ω^H using the relation $p = p^* + p'$;
13 Correct nodal and face velocity components on Ω^H (relations similar to Eqs. (14) and (15));
14 Correct mass fluxes on Ω^H applying velocity corrections on Eqs. (12) and (13);
15 Set $p^* = p$;
if $H = h$ **then**
16 Return solutions u, v and p and exit program;
else
17 Prolong u, v and p to the next fine grid $\Omega^{H/2}$;
18 $H \leftarrow H/2$;

In this work, before starting the execution of Algorithm 3, the velocity and pressure fields, as well as their respective corrections, are initialized as being null.

3.3. MG components and parameters

The general philosophy behind this work is to provide a model that is built on simple techniques and methods and yet still offers performances comparable to those in the literature. This way, as the next paragraphs show, all the methods and techniques employed in the construction of the numerical model are very common and many of them can be considered standard in the literature.

Regarding the MG method, the following parameters and components are used: the restriction operators used for the variables and residuals are the mean and the sum of correspondent fine volumes, respectively; for the mass fluxes, the restriction operator calculates the mass flux through a given coarse grid face as the sum of the fluxes through the two fine grid faces that correspond to it [2]; the bilinear operator is used for the prolongation of all variables and quantities, including the FMG prolongation of the converged solutions; standard coarsening ratio $q = 2$ is adopted; the maximum number of grid levels, $L_{\max}$, is used in both (u, v)-cycle and p-cycle; both (u, v)-cycle and p-cycle are executed only once in each Mod-SIMPLEC iteration, that is, $\gamma_1 = \gamma_2 = 1$; the number of relaxations (or inner iterations) performed in both pre- and post-smoothing phases is $\nu_1 = \nu_2 = 1$; the Gauss–Seidel solver with red-black ordering [26] is used for all systems of equations and in both cycles.

The stopping criteria used here to define the convergence of Mod-SIMPLEC, on each FMG level, are based on residuals and velocity errors. Following the recommendation of Kim *et al.* [30], the relative forms of the global residuals are used. The relative global residuals of the velocities are given by:

$$\bar{R}_\phi = \frac{\sum_P \left| A_P^V \phi_P - \sum_{nb} A_{nb}^V \phi_{nb} - S_P^\phi \right|}{\sum_P |A_P^V \phi_P|}, \tag{23}$$

where $\phi = u, v$. The relative global pressure-correction residuals are calculated as:

$$\bar{R}_p = \frac{\sum_P \left| (u_w - u_e)\Delta y + (v_s - v_n)\Delta x \right|}{\rho u_{\text{ref}} L_{\text{ref}}}, \tag{24}$$

where u_{ref} is a reference value of the u velocity and L_{ref} is a representative length of the cavity. For the classical problem [1], $u_{\text{ref}} = 1$ is adopted, that is, the prescribed top lid horizontal velocity. For the problem with manufactured solution [21], u_{ref} is taken as the average of the prescribed velocity distribution on the top lid, Eq. (4). As the cavity is square and unitary, the representative length is taken as $L_{\text{ref}} = 1$ for both problems.

The global errors of the velocities, indicated by e^u and e^V, are calculated in relation to the exact solutions of the problems. Exact solutions are considered to be those without iteration errors, that is, those obtained when external iterations (Mod-SIMPLEC iterations) are performed until the round-off error is reached. These solutions are indicated by ϕ^∞ and the related global errors are computed as:

$$e^\phi = \frac{\sum_P \left| \phi_P - \phi_P^\infty \right|}{NV}, \tag{25}$$

for $\phi = u, v$. Here, NV means the number of volumes. The error associated with the pressure field is not used in this case, since, as the motion equations are driven by pressure gradients,

different converged pressure fields can lead to the same velocity field. As can be noted from Eqs. (23)–(25), the residuals and errors are all represented by their respective relative l_1-norms.

Mod-SIMPLEC convergence, on each FMG level, is measured by the total global residual, R^T, and by the total global error, e, which are computed as:

$$R^T = \frac{\bar{R}_u + \bar{R}_v + \bar{R}_p}{3}, \quad e = \frac{e^u + e^v}{2}. \tag{26}$$

The tolerances for these quantities are indicated by ϵ_R and ϵ_e, respectively. For the classical problem, their values are taken to be $\epsilon_R = 5 \times 10^{-6}$ and $\epsilon_e = 10^{-6}$, and for the problem with analytical solutions, they are taken as $\epsilon_R = 10^{-7}$ and $\epsilon_e = 10^{-6}$.

The parameters and components adopted here are by no means fixed to the numerical model. The researchers who intend to employ this approach to the FMG-SIMPLEC algorithm are free to substitute these components with most advanced and efficient ones and/or with the ones they are experienced with.

4. Results

The results obtained with the numerical model developed from the proposed FMG-SIMPLEC approach are discussed in this section. The quality of the solutions, the associated errors and the MG performance are presented and analyzed. All the results associated with the developed model are indicated by the label "Mod-SIMPLEC." To minimize space in figures and tables, from this point onwards, the abbreviated forms "SG" and "MG" are used to refer to the terms "single grid" and "MG", respectively.

4.1. Code verification

4.1.1. Error analysis

The numerical error (E) associated with a certain variable is given by the difference between its exact analytical solution ($\bar{\phi}$) and its approximate numerical value (ϕ), i.e.,

$$E(\phi) = \bar{\phi} - \phi. \tag{27}$$

In absence of errors caused by truncation, iteration and round-off, the numerical error is called a discretization error [31]. In Marchi *et al.* [32], there is a study that seeks to reduce the discretization errors arising from various types of CFD problems through the use of polynomial interpolation followed by repeated Richardson extrapolation.

Considering the discretization methods and approximations used in this work (CDS and UDS with deferred correction in space), the predicted asymptotic order (p_L) of the discretization error must be equal to 2, that is, the numerical model as whole must achieve second-order accuracy [25]. The effective (p_E) and the apparent orders (p_U) are estimates to the asymptotic order and are calculated based on the numerical solutions. If h is the representative length of the grid, $h = \max(\Delta x, \Delta y)$, then, $p_E \to p_L$ and $p_U \to p_L$ when $h \to 0$. According to Marchi *et al.* [18], the effective and the apparent orders can be obtained, respectively, through the following relations:

$$p_E = \frac{\log\left[\frac{E(\phi_2)}{E(\phi_1)}\right]}{\log q}, \tag{28}$$

$$p_U = \frac{\left(\frac{\phi_2 - \phi_3}{\phi_1 - \phi_2}\right)}{\log q}, \tag{29}$$

where ϕ_1, ϕ_2, and ϕ_3 are the numerical solutions obtained on three grids coarsened in sequence with standard coarsening ratio $q = 2$, that is, with representative lengths h, $2h$, and $4h$, respectively. To use Eq. (28), the discretization error E, Eq. (27), must be known and, hence, the analytical solution is also necessary. Thus, for a problem without available analytical solution the effective order cannot be obtained and the asymptotic order must be estimated through the apparent order, Eq. (29).

The effective and the apparent orders of the discretization errors are analyzed for the following variables (ϕ) of interest: minimum value of u velocity along the vertical line $x = 1/2$ ($u_{\min}$); minimum and maximum values of v along the horizontal line $y = 1/2$ ($v_{\min}$ and $v_{\max}$, respectively); values of u and v at the center of the cavity (u_{center} and v_{center}); mass flow rate through the horizontal line $y = 1/2$ between points $x = 0$ and $x = 1/2$ (M_f); viscous drag force exerted by the fluid on the base of the cavity (F_s).

The values of u_{center} and v_{center} are calculated using the average mean of nodes adjacent to the cavity center. The analytical formulas of M_f and F_s and their corresponding numerical approximations can be checked in Marchi *et al.* [18]. In addition to these variables, the global discretization errors are also analyzed for the problem with analytical solution [21]. Using the l_1-norm, they are computed as:

$$E^{\phi} = \frac{\sum_P \left|\phi_P - \bar{\phi}_P\right|}{NV}, \tag{30}$$

for $\phi = u, v, p$.

The behavior of the effective orders of the discretization error with grid refinement can be observed in Figure 4. As the analytical solution is required for the calculation of these orders (Eq. (28)), the problem of Shih *et al.* [21] is used in this case. It is noted that both the orders of the global discretization errors of u, v and p (Figure 4*a*), and of the other variables of interest (Figure 4*b*), tend to the expected value 2 with grid refinement. As stated in the reference, $Re = 1$ for this problem.

In the case of apparent order (p_U), the values of the variables of interest for some values of Re in the classical problem are listed Table 1. The orders shown in this table are calculated in a $1{,}024^2$ grid, so the grids for ϕ_1, ϕ_2, and ϕ_3, in Eq. (29), have dimensions $1{,}024^2$, 512^2, and 256^2, respectively. Analyzing the values from table, it can be affirmed that most of the values are close to the expected value 2. The values of the apparent orders are quite sensitive to the methods used in the calculation of the involved variables, especially those obtained from formulas based on averages or numerical integration. This way, perhaps the apparent orders of $v_{\min}$ and v_{center},

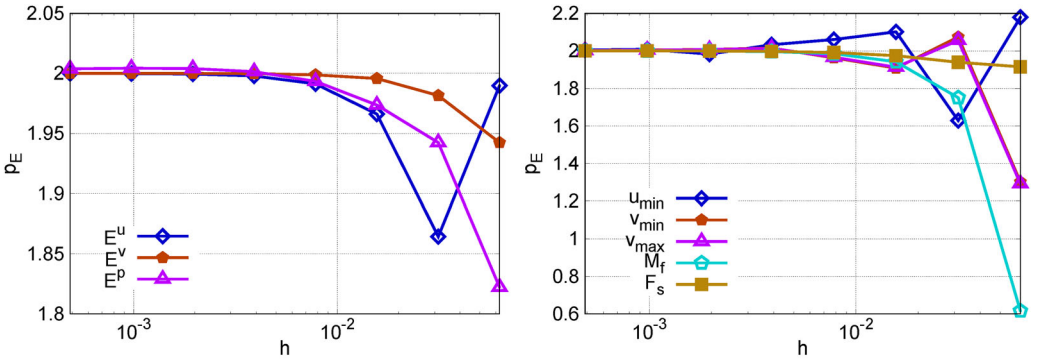

(*a*) u, v and p global discretization errors. (*b*) Errors of some variables of interest.

Figure 4. Behavior of effective orders (p_E) with grid refining ($h \to 0$) for the problem of Shih *et al.* [21].

for $Re = 100$, could reach more adequate values if these variables were calculated using alternative forms. Similar results can be found in Marchi *et al.* [18].

4.1.2. Numerical solutions

The accuracy of the solutions can be assessed qualitatively in Figures 5 and 6. In Figure 5, comparisons of velocities and pressure profiles with their correspondent analytical solutions along the cavity center lines can be observed. As can be inferred, in all cases, there is good correspondence between the generated solutions and their analytical counterparts. In Figure 6, the center profiles of the velocities, obtained from the classical problem, are presented for some Reynolds number values. These profiles are compared with results from Roy *et al.* [14], Erturk [19], and Marchi *et al.* [18]. Again, it can be noted that all the produced profiles are in well agreement with their

Table 1. Apparent orders (p_U) of variables of interest in the classical problem.

	$Re = 100$	$Re = 400$	$Re = 1,000$
u_{min}	2.07441	2.03095	1.99649
v_{min}	1.11741	2.14317	2.12429
v_{max}	1.86029	2.01725	1.97254
u_{center}	1.99748	2.01548	2.08039
v_{center}	1.37616	2.01469	2.38602
M_f	2.00122	2.00748	2.00144
F_s	2.00352	1.65285	1.92807

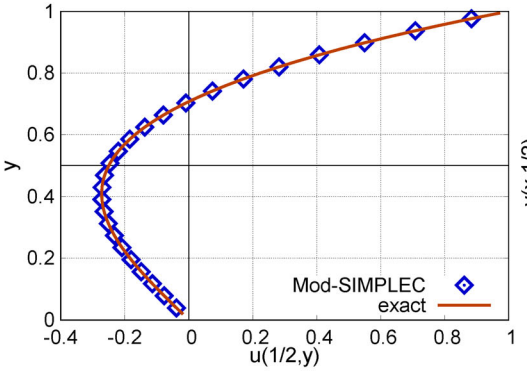

(*a*) u-velocity profile along the vertical center line $x = 1/2$.

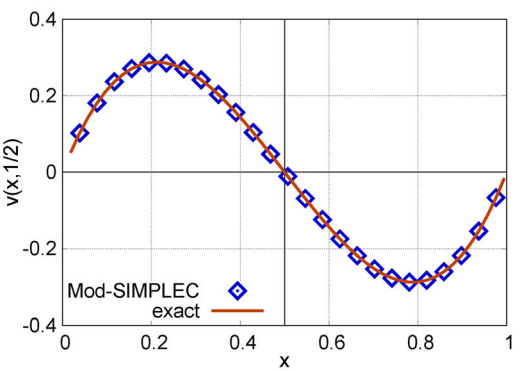

(*b*) v-velocity profile along the horizontal center line $y = 1/2$.

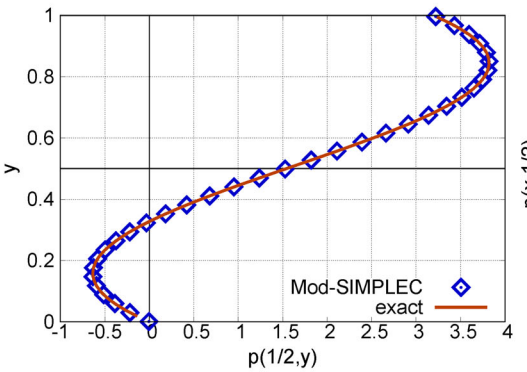

(*c*) Pressure (p) profile along the vertical center line $x = 1/2$.

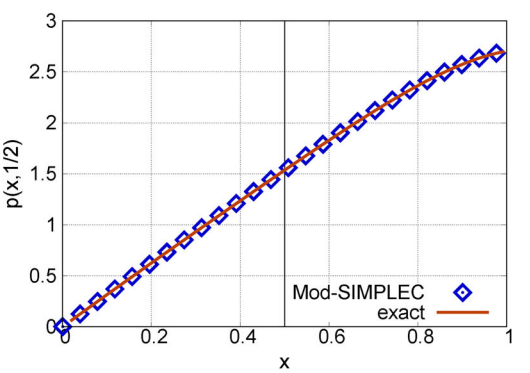

(*d*) Pressure (p) profile along the horizontal center line $y = 1/2$.

Figure 5. Velocities and pressure profiles along the center lines of the cavity for the problem of Shih *et al.* [21].

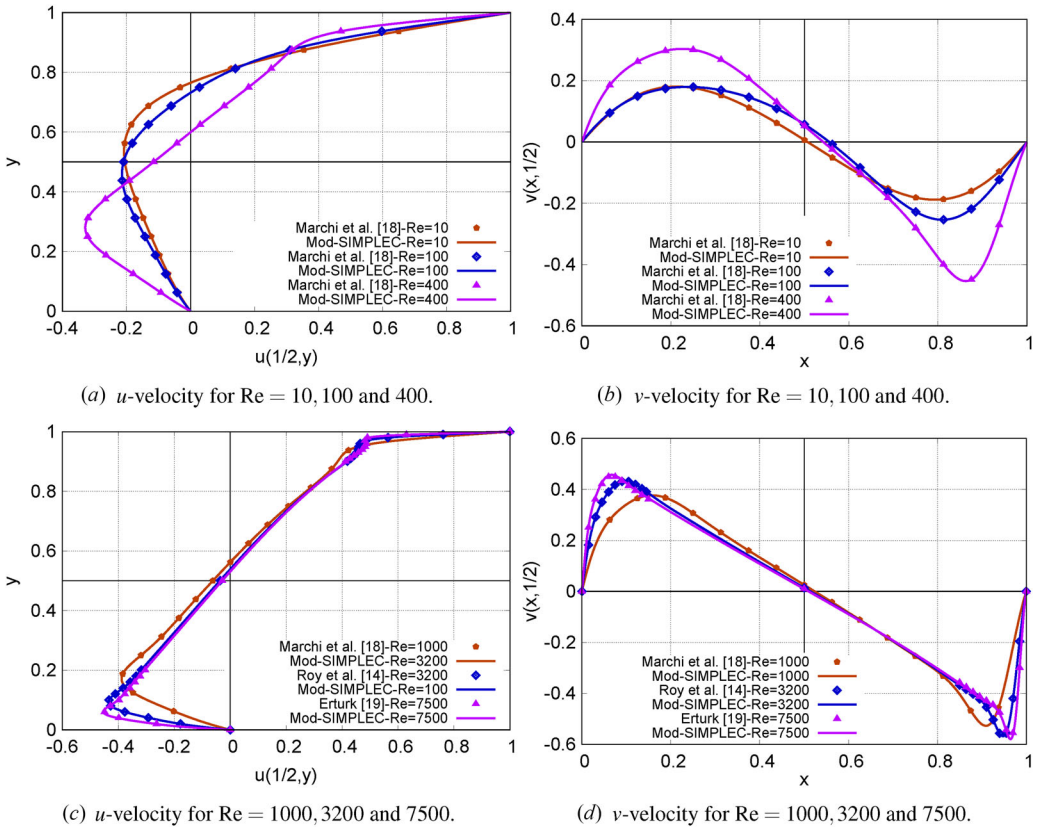

(*a*) *u*-velocity for Re = 10, 100 and 400.

(*b*) *v*-velocity for Re = 10, 100 and 400.

(*c*) *u*-velocity for Re = 1000, 3200 and 7500.

(*d*) *v*-velocity for Re = 1000, 3200 and 7500.

Figure 6. Velocities profiles along the center lines of the cavity for some Reynolds values in the classical problem.

correspondents from the references. These works also compare their results with those from Ghia *et al.* [1], Bruneau and Saad [33], and Botella and Peyret [34]. This way, the present results are also in well agreement with those.

The streamlines of the classical problem for higher values of *Re* (with the exception of $Re = 400$) are presented in Figure 7. Qualitatively, it can be stated that the patterns of streamlines and central vortices (primary) and cavity corners (secondary, tertiary, etc.) are consistent with the literature [13,19].

In Table 2, the values of the same variables of interest of Table 1 can be compared with the ones from Marchi *et al.* [18]. As can be seen, the values are in good agreement. All these profiles and results were generated in a grid with dimension $1{,}024^2$.

4.2. Performance of the alternative FMG-SIMPLEC approach

As mentioned in Subsection 4.1.1, the discretization error can only be calculated when the analytical solution is available, as is the case with the problem of Shih *et al.* [21]. Figure 8 shows the decay of total global residuals and errors with the number of iterations (it) for this problem.

The first point to be noted is that the adopted stopping criteria and associated tolerances are adequate, since, in both SG and MG methods, the tolerances $\epsilon_R = 10^{-7}$ and $\epsilon_e = 10^{-6}$ guarantee the convergence of the true discretization errors, E^{ϕ} ($\phi = u, v, p$). It is also observed that approximately 10^4 iterations are required for the (total global) error convergence in the SG method. In the case of the MG method, a much smaller number, approximately 130 iterations, is required

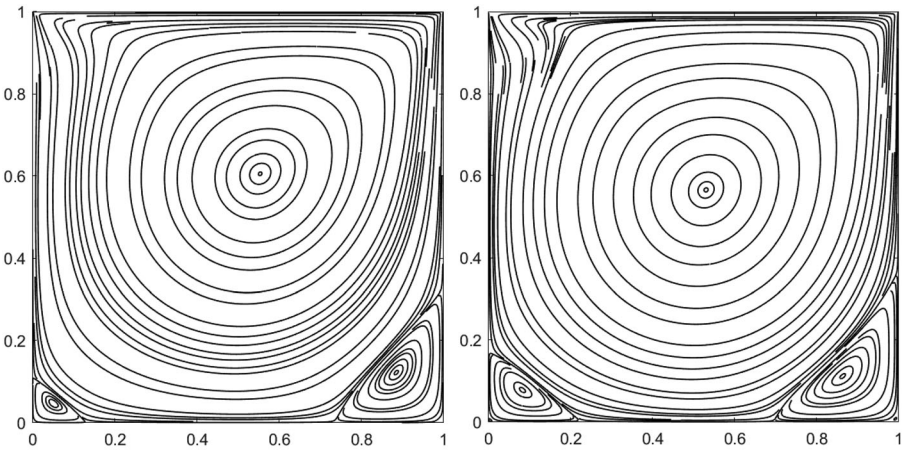

(*a*) Re = 400 (*b*) Re = 1000

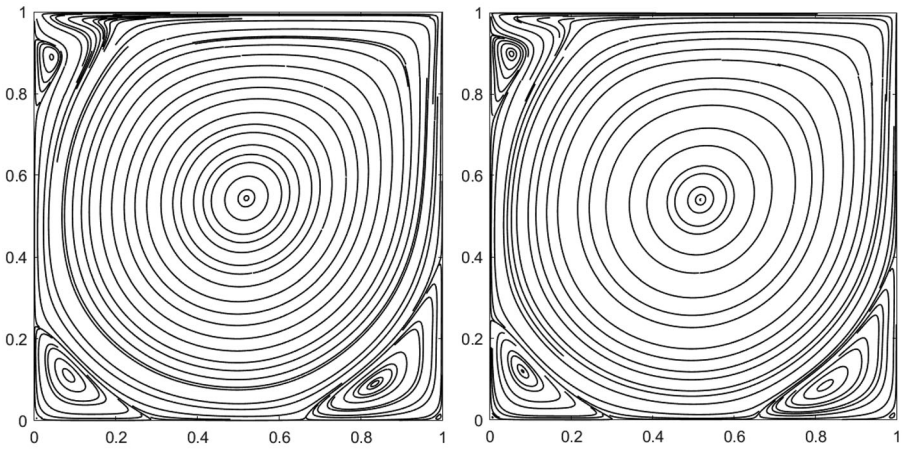

(*c*) Re = 2500 (*d*) Re = 3200

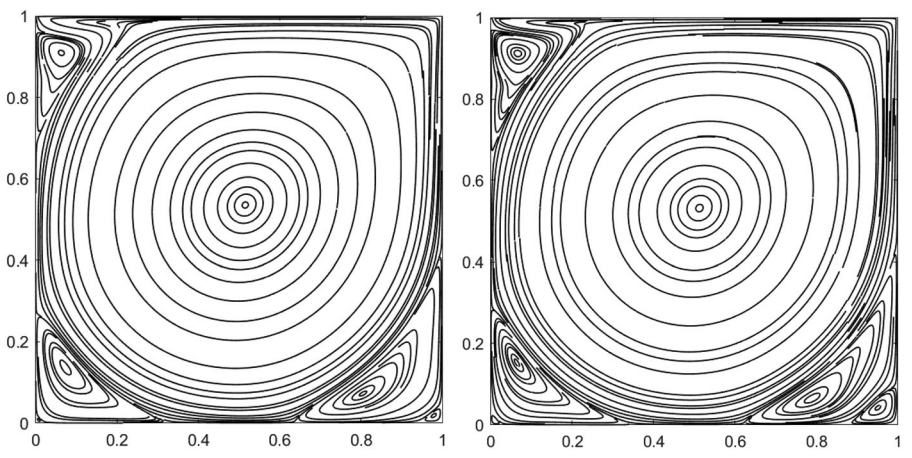

(*e*) Re = 5000 (*f*) Re = 7500

Figure 7. Streamlines of the classical problem.

Table 2. Variables of interest in the classical problem.

	$Re = 100$		$Re = 400$		$Re = 1,000$	
Variable	Mod-SIMPLEC	[18]	Mod-SIMPLEC	[18]	Mod-SIMPLEC	[18]
u_{min}	−0.214042	−0.214036	−0.328730	−0.328695	−0.388572	−0.388470
v_{min}	−0.253804	−0.253799	−0.454058	−0.454021	−0.527056	−0.526940
v_{max}	0.179573	0.179569	0.303832	0.303800	0.376947	0.376850
u_{center}	−0.209149	−0.209143	−0.115054	−0.115052	−0.0620561	−0.0620503
v_{center}	0.0575366	0.0575367	0.0520581	0.0520631	0.0257995	0.0258001
M_f	0.0665473	0.0665461	0.106628	0.106620	0.116514	0.116490
F_s	0.00326793	0.00326798	0.00119435	0.00119434	0.000798040	0.000797840

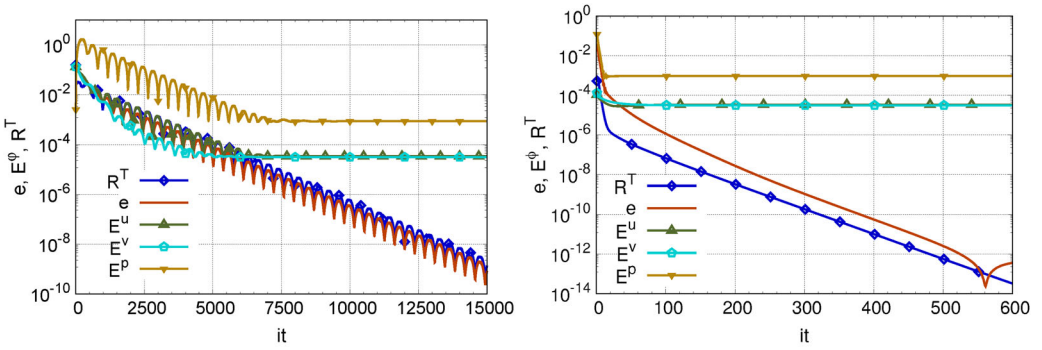

(*a*) SG method. (*b*) MG method.

Figure 8. Decay of residuals and discretization errors in the Navier–Stokes equations (problem of Shih).

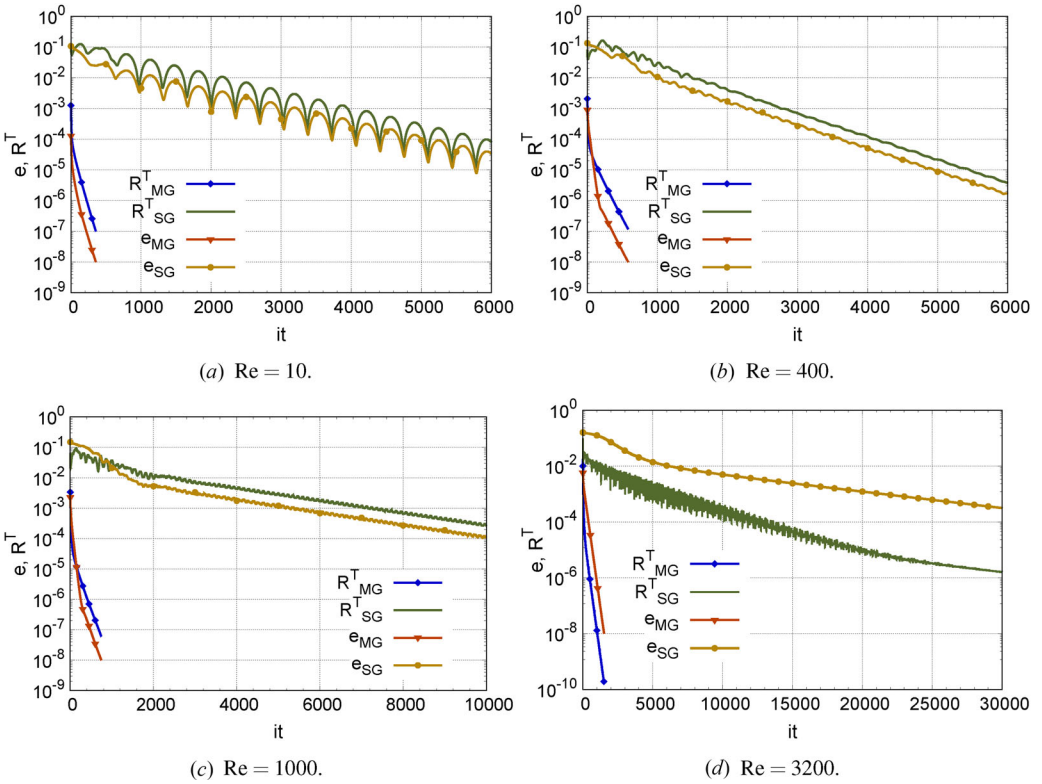

(*a*) Re = 10. (*b*) Re = 400.

(*c*) Re = 1000. (*d*) Re = 3200.

Figure 9. Decay of residuals and discretization errors in the Navier–Stokes equations (classical problem).

for the convergence of the error. The initial fine grid had dimension 256^2 in these cases. Finer grids would imply very high numbers of iterations for the SG method, making performance analysis difficult.

Total global residuals and errors decays for the classical problem are shown in Figure 9. In all cases, the error and residual decay rates of the MG are much higher when compared to those of the SG. For $Re = 1,000$, for example, the number of iterations (it) necessary for R^T and e to fall bellow their given tolerances is $O(10^2)$ for the MG method. For the SG method, as the graphical trend indicates, this number is (at least) $O(10^4)$.

The apparent high number of iterations required for the MG residuals and errors to fall below their tolerances is due to the pseudo-time-marching formulation, which must converge from an initial (pseudotransient) state to a steady-state solution in each case. A similar behavior can be observed in Chen *et al.* [35], where this under-relaxation technique is also used in conjunction with the MG. Another issue that contributes to this behavior is the fact that the number of inner iterations (relaxations) performed in each solver is equal to unity in all cases; thus, more external (Mod-SIMPLEC) iterations are necessary. It can be concluded, therefore, that alternative ways of evaluating the MG performance, which are not based only on the number of external iterations, should be used for the numerical model presented in this work.

In Trottenberg *et al.* [26], it is affirmed that time is a good parameter to measure the performance of MG numerical models. According to Brandt [10], *apud* Roy *et al.* [14], the "golden rule" of MG methods, translated in terms of computational time, states that the time should increase linearly with the number of grid nodes (N), that is, it should exhibit an $O(N)$ increase. This way, the next results use time as the main parameter to compare the performances of the SG and MG methods.

In Table 3, SG and MG execution times from Mod-SIMPLEC are presented, together with the respective speedups (S), for some Reynolds values in the classical problem and also for $Re = 1$ in the problem of with analytical solution (the notation "*" is used in this case). Results in this format are generally found in literature only for a limited range of Re values. A good performance is observed for ${}^*Re = 1$ and also for $Re = 10$ in the classical problem (mainly in the 512^2 grid). The speedups are less expressive for $Re = 400$ and seem to improve again for $Re = 1,000$. For higher Re values, 2,500 and 3,200, the speedups follow the orders of magnitude, of the other Re values, up to the 512^2 grid. In the $1{,}024^2$ grid, however, a drop in performance can be observed. In Roy *et al.* [14], it is stated that the large convection effects, related to higher Re numbers, can compromise the accuracy of the prolongation of converged coarse grid solutions to the next finer grids. Thus, according to the authors, a good initial estimate for the next finer (FMG) level may not be possible to achieve in these flow regimes.

Mod-SIMPLEC execution times from Tab. 3, and also for other Re values, are plotted versus NV in Figure 10. The light gray lines, indicated by the legend "linear," represent the linear

Table 3. CPU times (s) from Mod-SIMPLEC and related speedups (S).

	${}^*Re = 1$			$Re = 10$			$Re = 400$		
Grid	SG	MG	S	SG	MG	S	SG	MG	S
64^2	1.086	0.049	22.16	1.066	0.042	25.38	0.925	0.062	14.92
128^2	12.355	0.239	51.69	6.963	0.236	29.50	8.467	0.343	24.68
256^2	193.677	1.341	144.43	108.643	1.502	72.33	99.285	2.306	43.05
512^2	3,010.880	7.646	393.78	1,757.160	9.403	186.87	1,756.730	16.559	106.09
$1{,}024^2$	46,809.100	29.805	1,570.51	28,410.000	29.142	974.88	30,981.200	54.141	572.23
	$Re = 1,000$			$Re = 2,500$			$Re = 3,200$		
Grid	SG	MG	S	SG	MG	S	SG	MG	S
64^2	2.153	0.146	14.75	4.895	0.532	9.20	5.839	0.868	6.73
128^2	18.537	0.587	31.58	49.604	2.061	24.07	77.511	3.253	23.83
256^2	185.392	2.844	66.19	675.662	8.356	80.86	1,207.060	12.450	96.95
512^2	2,975.053	15.493	192.03	6,140.354	37.234	164.91	9,696.710	53.629	180.79
$1{,}024^2$	47,515.800	68.749	691.15	56,246.400	146.916	382.85	79,034.900	208.267	379.49

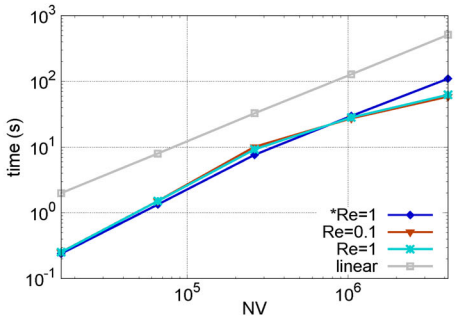

(*a*) Problem of Shih: *Re = 1. Classical problem: Re = 0.1 and Re = 1.

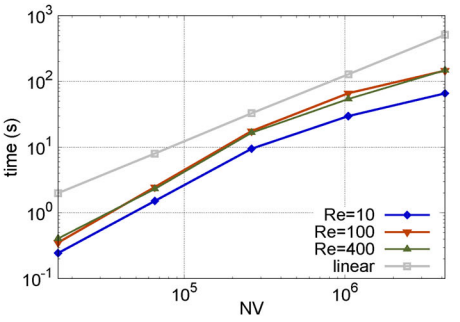

(*b*) Classical problem: Re = 10, Re = 100 and Re = 400.

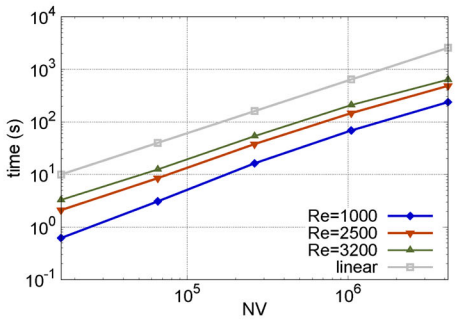

(*c*) Classical problem: Re = 1000, Re = 2500 and Re = 3200.

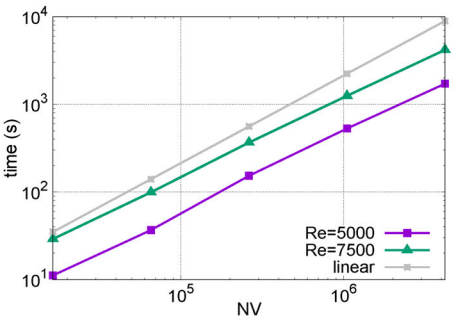

(*d*) Classical problem: Re = 5000 and Re = 7500.

Figure 10. Mod-SIMPLEC performance: execution times *versus* the number of grid volumes (*NV*).

Table 4. Mod-SIMPLEC complexity orders (*p*) for the Navier–Stokes under some *Re* values.

	$\hat{*}Re = 1$	$Re = 0.1$	$Re = 1$	$Re = 10$	$Re = 100$	$Re = 400$
p	1.07	1.00	1.01	1.02	1.11	1.13
	$Re = 1,000$	$Re = 2,500$	$Re = 3,200$	$Re = 5,000$	$Re = 7,500$	
p	1.09	0.99	0.96	0.90	0.90	

relationship between the execution times and *NV*, that is, they represent the MG expected behavior according to Brandt [10] *apud* Roy *et al.* [14].

In most curves, there is a slope decrease from grid 512^2, and from that point on the curves indicate the presence of an approximately linear, or even sublinear, time growth pattern. These changes in the slopes are more evident for $Re \leq 1000$; for higher values, they are more subtle and the curves appear to be subject to more constant slopes. Moreover, this sublinear time growth regime, assumed by most curves, indicates that the Mod-SIMPLEC performance tends to improve with the use of increasingly refined grids.

Finally, the slopes (*p*) of the straight lines that best fit the curves in Figure 10 are listed in Table 4. They represent the order (or complexity order) of the solver and are a measure of the computational effort of the method. The ideal MG behavior requires that *p* be unitary, indicating that time increases linearly with the number os volumes (light gray lines in Figure 10). Unfortunately, for $Re = 100$ and $Re = 400$, where much of the data for benchmarking if found in literature, the method presents the weakest performances. This is in accordance with the low speedups performances for $Re = 400$ in Table 3. Still, *p* values are not far from unity in these cases and as, aforementioned, according to

Figure 10, the curves indicate that the ideal behavior could be reached if more refined grids were used.

In general, it is noted that the value of p is close to unity in all cases. Therefore, it can be concluded that Archi Brandt's "golden rule," as pointed out by Roy *et al.* [14], is practically satisfied for most of the simulated regimes. Furthermore, the developed model effectively achieves the desired performance rule precisely where the literature lacks data, i.e. for higher Reynolds number values.

5. Conclusions

In this work, an alternative approach was presented to employ the FMG-SIMPLEC (full MG SIMPLEC) algorithm to solve the steady-state incompressible Navier–Stokes equations. The FMG algorithm is based on a modified SIMPLEC algorithm (Mod-SIMPLEC) that preserves all original SIMPLEC steps, with the exception of the steps associated with the resolution of the linear systems. In Mod-SIMPLEC, these steps use independent V-cycles to solve the systems. The discretization methods and approximations techniques used for the original mathematical model allow the generated numerical scheme to use two independent V-cycles on each FMG level: one to solve the momentum equations, called (u, v)-cycle, and another to solve the pressure-correction equation, called p-cycle. Thus, in Mod-SIMPLEC, all the other original SIMPLEC steps may be executed only on the finest grid of each FMG level. The other intermediate coarse grids are used only internally in these V-cycles to smooth the errors of the corresponding systems.

The lid-driven flow in the unitary square cavity was used as the model problem in two variants: the classical cavity problem, with uniform unitary horizontal velocity on the top lid [1]; and the problem with a manufactured analytical solution from Shih *et al.* [21]. In terms of the quality of the solutions, the developed numerical model produced velocity fields very close to those of the literature for the classical problem, even for high values of Re, and also results that agreed very well with their analytical counterparts, with the associated errors satisfying the expected behavior of error analysis theory.

Despite the simplicity of the proposed approach, several tests have shown that its performance is comparable to the standard MG-SIMPLE-like approaches found in literature, with speedups orders of magnitude as high as $O(10^3)$ being obtained. But, above all, the tests also showed that Brandt's MG performance criterion, in terms of execution times, was generally met for all values of Re used in the simulations, but mainly, and effectively, for high values of Re. For intermediate values, the results showed that the linear (or sublinear) trend was observed for more refined grids (from 512^2 grids). As stated at the beginning of the text, the objective here was to offer an alternative approach that allows the construction of numerical models with a simple and easy to implement structure and still benefits from the performance gains associated with MG methods. Thus, it can be said that this goal has been successfully achieved for a wide range of Re numbers.

Finally, an important feature of the presented approach concerns the fact that it is not fixed and, thereby, can be constructed with different schemes and techniques, such as discretization schemes of higher order, schemes other than MIM to interpolate face velocities, different transfer operators and solvers, and so on. Thus, researchers can compose their Mod-FMG models according to their preferences, whether focusing on performance, accuracy, or other desired features.

Disclosure statement

The authors declare that there are no conflicts of interest related to this study.

Funding

The authors would like to thank the financial support for this work provided by the Coordenação de Aperfeiçoamento de Pessoal de Nível Superior - Brasil (CAPES) - Finance Code 001. They also acknowledge the Graduate Program in Numerical Methods in Engineering (PPGMNE) and the infrastructure of the Numerical Experimentation Laboratory (LENA) of the Federal University of Parana (UFPR). The authors declare that no specific funding was received for this study.

ORCID

Jean Michael Borges de Oliveira http://orcid.org/0000-0002-8823-9432
Luciano Kiyoshi Araki http://orcid.org/0000-0003-0130-739X
Marcio Augusto Villela Pinto http://orcid.org/0000-0003-4166-4674
Simone de Fátima Tomazzoni Gonçalves http://orcid.org/0000-0003-3953-0327

References

[1] U. Ghia, K. N. Ghia, and C. T. Shin, "High-resolutions for incompressible flow using the Navier–Stokes equations and a multigrid method," *J. Comput. Phys.*, vol. 48, no. 3, pp. 387–411, 1982. DOI: 10.1016/0021-9991(82)90058-4.

[2] M. Hortmann, M. Perić, and G. Scheuerer, "Finite volume multigrid prediction of laminar natural convection: Bench-mark solutions," *Int. J. Numer. Meth. Fluids*, vol. 11, no. 2, pp. 189–207, Jul. 1990. DOI: 10.1002/fld.1650110206.

[3] E. Erturk, T. C. Corke, and C. Gökçöl, "Numerical solutions of 2-D steady incompressible driven cavity flow at high Reynolds numbers," *Int. J. Numer. Meth. Fluids*, vol. 48, no. 7, pp. 747–774, 2005. DOI: 10.1002/fld.953.

[4] A. S. Kozelkov, S. V. Lashkin, A. A. Kurkin, A. V. Kornev, and A. M. Vyalykh, "An efficient parallel implementation of the SIMPLE algorithm based on a multigrid method," *Numer. Anal. Appl.*, vol. 13, no. 1, pp. 1–16, 2020. DOI: 10.1134/S1995423920010012.

[5] F. S. Lien and M. A. Leschziner, "Multigrid acceleration for recirculating laminar, and turbulent flows computed with a non-orthogonal, collocated finite-volume scheme," *Comput. Methods Appl. Mech. Eng.*, vol. 118, no. 3–4, pp. 351–371, 1994. DOI: 10.1016/0045-7825(94)90007-8.

[6] S. V. Patankar and D. B. Spalding, "A calculation procedure for heat, mass and momentum transfer in three-dimensional parabolic flows," *Int. J. Heat Mass Transfer*, vol. 15, no. 10, pp. 1787–1806, 1972. DOI: 10.1016/0017-9310(72)90054-3.

[7] M. Anunciação, M. A. V. Pinto, and L. A. Neundorf, "Solution of the Navier–Stokes equations using projection method and preconditioned conjugated gradient with multigrid and ILU solver," *RIMNI.*, vol. 36, no. 1, pp. 1–25, 2020. DOI: 10.23967/j.rimni.2020.01.003.

[8] R. Fedorenko, "The speed of convergence of one iterative process," *USSR Comput. Math. Math. Phys.*, vol. 4, no. 3, pp. 227–235, Jan. 1964. DOI: 10.1016/0041-5553(64)90253-8.

[9] N. Bakhvalov, "On the convergence of a relaxation method with natural constraints on the elliptic operator," *USSR Comput. Math. Math. Phys.*, vol. 6, no. 5, pp. 101–135, Jan. 1966. DOI: 10.1016/0041-5553(66)90118-2.

[10] A. Brandt, "Multi-level adaptive solutions to boundary-value problems," *Math. Comp.*, vol. 31, no. 138, pp. 333–390, May 1977. DOI: 10.1090/S0025-5718-1977-0431719-X.

[11] U. Trottenberg and K. Stüben, "Multigrid methods: Fundamental algorithms, model problem analysis and applications," in *Multigrid Methods*, Lecture Notes in Mathematics, vol. 960, W. Hackbusch and U. Trottenberg, Eds. Berlin, Heidelberg: Springer, 1982, pp. 1–176. DOI: 10.1007/BFb0069928.

[12] J. H. Ferziger, M. Perić, G. Scheuerer, and C. Becker, "Finite volume multigrid solutions of the two-dimensional incompressible Navier–Stokes-equations," in *Robust Multi-Grid Methods*, ser. Notes on Numerical Fluid Mechanics, vol. 23. Wiesbaden, Germany: Vieweg & Teubner Verlag, 1989, pp. 37–47.

[13] S. K. Kumar, S. D. Kumar, and M. Kumar, "A fine grid solution for a lid-driven cavity flow using multigrid method," *Eng. Appl. Comput. Fluid Mech.*, vol. 3, no. 3, pp. 336–354, 2009.

[14] P. Roy, N. K. Anand, and D. Donzis, "A parallel multigrid finite-volume solver on a collocated grid for incompressible Navier–Stokes equations," *Numer. Heat Transf. B: Fundam.*, vol. 67, no. 5, pp. 376–409, 2015. DOI: 10.1080/10407790.2014.985980.

[15] C. M. Rhie and W. L. Chow, "Numerical study of the turbulent flow past an airfoil with trailing edge separation," *AIAA J.*, vol. 21, no. 11, pp. 1525–1532, 1983. DOI: 10.2514/3.8284.

[16] D. K. Kolmogorov, W. Z. Shen, N. N. Sorensen, and J. N. Sorensen, "Fully consistent SIMPLE-like algorithms on collocated grids," *Numer. Heat Transf. B: Fundam.*, vol. 67, no. 2, pp. 101–123, 2015. DOI: 10.1080/10407790.2014.949583.

[17] J. Yan, F. Thiele, and L. Xue, "A modified full multigrid algorithm for the Navier–Stokes equations," *Comput. Fluids*, vol. 36, no. 2, pp. 445–454, Feb. 2007. DOI: 10.1016/j.compfluid.2006.01.017.

[18] C. H. Marchi, R. Suero, and L. K. Araki, "The lid-driven square cavity flow: Numerical solution with a 1024 x 1024 grid," *J. Braz. Soc. Mech. Sci. Eng.*, vol. 31, no. 3, pp. 186–198, Sept. 2009. DOI: 10.1590/S1678-58782009000300004.

[19] E. Erturk, "Discussions on driven cavity flow," *Int. J. Numer. Meth. Fluids*, vol. 60, no. 3, pp. 275–294, 2009. DOI: 10.1002/fld.1887.

[20] M. Kawaguti, "Numerical solution of the Navier–Stokes equations for the flow in a two-dimensional cavity," *J. Phys. Soc. Jpn.*, vol. 16, no. 11, pp. 2307–2315, 1961. DOI: 10.1143/JPSJ.16.2307.

[21] T. M. Shih, C. H. Tan, and B. C. Hwang, "Effects of grid staggering on numerical schemes," *Int. J. Numer. Meth. Fluids*, vol. 9, no. 2, pp. 193–212, Feb. 1989. DOI: 10.1002/fld.1650090206.

[22] C. R. Maliska, *Heat Transfer and Computational Fluid Mechanics (in Portuguese)*, 2nd ed. Rio de Janeiro, Brazil: LTC, 2004.

[23] S. G. Rubin and P. K. Khosla, "Polynomial interpolation methods for viscous flow calculations," *J. Comput. Phys.*, vol. 24, no. 3, pp. 217–244, 1977. DOI: 10.1016/0021-9991(77)90036-5.

[24] R. L. Burden and J. D. Faires, *Numerical Analysis*, 9th ed. Boston, USA: Brooks/Cole, 2011,

[25] J. H. Ferziger and M. Perić, *Computational Methods for Fluid Dynamics*, 3rd ed. Berlin, Heidelberg: Springer-Verlag, 2002.

[26] U. Trottenberg, C. Osterlee, and A. Schuller, *Multigrid*. New York, NY: Academic Press, 2001,

[27] A. Brandt and O. E. Livne, *Multigrid Techniques: 1984 Guide with Applications to Fluid Dynamics*, Revised Edition, ser. Classics in Applied Mathematics, vol. 67. Philadelphia, USA: SIAM, 2011.

[28] A. Thekale, T. Gradl, K. Klamroth, and U. Rüde, "Optimizing the number of multigrid cycles in the full multigrid algorithm," *Numer. Linear Algebra Appl.*, vol. 17, no. 2–3, pp. 199–210, Feb. 2010. DOI: 10.1002/nla.697.

[29] C. D. Santiago, C. H. Marchi, and L. F. Souza, "Performance of geometric multigrid method for coupled two-dimensional systems in CFD," *Appl. Math. Modell.*, vol. 39, no. 9, pp. 2602–2616, 2015. DOI: 10.1016/j.apm.2014.10.067.

[30] N. Kim, N. L. Anand, and D. L. Rhode, "A study on convergence criteria for a SIMPLE-based finite-volume algorithm," *Numer. Hear Transf. B: Fundam.*, vol. 34, no. 4, pp. 401–417, 1998. DOI: 10.1080/10407799808915065.

[31] C. H. Marchi and A. F. C. Silva, "Unidimensional numerical solution error estimation for convergent apparent order," *Numer. Heat Transf. B: Fundam.*, vol. 42, no. 2, pp. 167–188, 2002. DOI: 10.1080/10407790190053888.

[32] C. H. Marchi *et al.*, "Polynomial interpolation with repeated Richardson extrapolation to reduce discretization error in CFD," *Appl. Math. Modell.*, vol. 40, no. 21–22, pp. 8872–8885, 2016. DOI: 10.1016/j.apm.2016.05.029.

[33] C. H. Bruneau and M. Saad, "The 2D lid-driven cavity problem revisited," *Comput. Fluids*, vol. 35, no. 3, pp. 326–348, 2006. DOI: 10.1016/j.compfluid.2004.12.004.

[34] O. Botella and R. Peyret, "Benchmark spectral results on the lid-driven cavity flow," *Comput. Fluids*, vol. 27, no. 4, pp. 421–433, 1998. DOI: 10.1016/S0045-7930(98)00002-4.

[35] W. Chen, Y. Ju, and C. Zhang, "A multidomain multigrid pseudospectral method for incompressible flows," *Numer. Heat Transf. B*, vol. 74, no. 1, pp. 415–431, 2018. DOI: 10.1080/10407790.2018.1490090.